Surface segregation at the aluminum interface of poly(3-hexylthiophene)/fullerene solar cells

Akiko Orimo,[1] Kohji Masuda,[1] Satoshi Honda,[1] Hiroaki Benten,[1] Shinzaburo Ito,[1] Hideo Ohkita,[2,a)] and Hiroshi Tsuji[3]
[1]*Department of Polymer Chemistry, Graduate School of Engineering, Kyoto University, Katsura, Kyoto 615-8510, Japan*
[2]*Department of Polymer Chemistry, Graduate School of Engineering, Kyoto University, Katsura, Kyoto 615-8510, Japan and PRESTO, Japan Science and Technology Agency (JST), 4-1-8 Honcho Kawaguchi, Saitama 332-0012, Japan*
[3]*Department of Electronic Science and Engineering, Graduate School of Engineering, Kyoto University, Katsura, Kyoto 615-8510, Japan*

(Received 27 November 2009; accepted 27 December 2009; published online 26 January 2010)

The effects of thermal annealing before and after Al deposition on poly(3-hexylthiophene) (P3HT)/[6,6]-phenyl-C_{61} butyric acid methyl ester (PCBM) blend solar cells were investigated by current density-voltage measurements and x-ray photoelectron spectroscopy (XPS). Compared to the preannealed device, the postannealed device exhibited enhanced open-circuit voltage (V_{OC}), which is ascribed to the decrease in the reverse saturation current density J_0. The XPS measurements demonstrated that P3HT is dominant at the Al interface in the preannealed device while PCBM is instead dominant in the postannealed device. This surface-segregated PCBM formed in the postannealed device can serve as a hole-blocking layer at the Al interface to reduce J_0, and therefore improve V_{OC}. © *2010 American Institute of Physics*. [doi:10.1063/1.3294290]

Polymer solar cells have attracted considerable attention because of their potential advantages such as light weight, flexibility, low-cost, and high-throughput productivity.[1] The blend of poly(3-hexylthiophene)(P3HT)/[6,6]-phenyl-C_{61} butyric acid methyl ester (PCBM) has been most intensively studied in recent years and exhibited a power conversion efficiency of 4–5%.[2] In such solar cells based on a blended active layer, the control of the blend morphology is critical for improving the device performance. Recently, vertical phase separation has been reported for a variety of conjugated polymer blend systems[3,4] including P3HT/PCBM.[5–7] In most cases, conjugated polymers with a lower surface energy have been reported to be segregated at the air interface. This finding suggests that the normal device structure would be unsuitable for selective electron collection at the top electrode such as Al with a low work function but rather the inverted device structure would be a more promising choice.[6,8] Nevertheless, P3HT/PCBM solar cells exhibit as mentioned above good performance for the normal device structure. In this letter, we report the effects of thermal annealing before and after Al deposition on P3HT/PCBM blend solar cells by current density-voltage (*J-V*) measurements and x-ray photoelectron spectroscopy (XPS). To address the origin of the significant improvement in the open-circuit voltage (V_{OC}) particularly, we focused our attention on the dependence of the surface composition at the Al electrode on the thermal annealing procedures.

Bulk heterojunction solar cells based on P3HT/PCBM blends were fabricated as follows. First, a thin layer of poly(3,4-ethylenedioxythiophene):poly(4-styrenesulfonate) (PEDOT:PSS) (40 nm) was spin-coated on an indium-tin-oxide-coated substrate (10 Ω/sq). Then, a blend layer of P3HT/PCBM (170 nm) was prepared on the PEDOT:PSS layer by spin-coating from a chlorobenzene solution of P3HT and PCBM (1:1 by weight). Finally, Al electrode (100 nm) was thermally deposited on top of the active layer at 2.5×10^{-6} Torr. The active layer was thermally annealed at 150 °C for 30 min in a nitrogen-filled glove box before (preannealing) or after (postannealing) the Al deposition. The *J-V* characteristics of the solar cells were measured under a nitrogen atmosphere with a dc voltage and current source/monitor in the dark and under the illumination with AM1.5G simulated solar light at 100 mW cm^{-2}. The samples for XPS analysis were fabricated by the same procedure as the device fabrication mentioned above. After the thermal annealing, the Al electrode partly deposited was removed with a diluted aqueous solution of NaOH and the exposed surface was rinsed with ultrapure water. The XPS measurement was performed in an ultrahigh vacuum system (Shimadzu–Kratos, AXIS 165). The XPS spectra were measured using an Al Kα radiation source ($h\nu$=1486.6 eV) for the sample surface without Al deposition (preannealing) and for the other surface after the removal of the Al electrode (postannealing).

As summarized in Table I, the postannealed device exhibited slightly improved short-circuit current density (J_{SC}) and fill factor (FF), and substantially enhanced V_{OC} from 0.4 to 0.6 V compared to the preannealed device. This is a typical change in the device performance of P3HT/PCBM solar cells under different annealing procedures as reported previously.[9] In general, the improvement in the device performance is explained in terms of better interfacial contact between the active layer and the Al electrode by postannealing. In this study, we focus our attention on the significant improvement in V_{OC}.

To address the origin of the improvement in V_{OC} by postannealing, we analyzed the *J-V* characteristics of the same devices in the dark using the equivalent circuit model as shown in the inset of Fig. 1. In this model, the *J-V* char-

a)Electronic mail: ohkita@photo.polym.kyoto-u.ac.jp.

TABLE I. Device performances and *J-V* characteristics parameters of P3HT/PCBM solar cells.

Anneal	J_{SC} (mA cm^{-2})	V_{OC} (V)	FF	PCE (%)	J_0 (A cm^{-2})	n	R_P (Ω)	R_S (Ω)
Pre	6.9	0.42	0.46	1.3	9.0×10^{-7}	2.0	8.0×10^{4}	100
Post	7.7	0.59	0.58	2.7	3.6×10^{-9}	1.7	3.5×10^{5}	35

acteristics can be derived by the following equation:[10]

$$J = J_0\left\{\exp\left[\frac{e(V-JAR_S)}{nk_BT}\right]-1\right\}+\frac{(V-JAR_S)}{R_PA}-J_{ph}, \quad (1)$$

where J_0 is the reverse saturation current density, n is the ideality factor, R_S is the series resistance, R_P is the parallel resistance, e is the elementary charge, k_B is the Boltzmann constant, T is the temperature, and A is the active area of the device. As shown in Fig. 1, the dark *J-V* characteristics are well fitted with Eq. (1). The fitting parameters are summarized in Table I. Assuming that J_{ph} is equal to J_{SC}, Eq. (1) is simplified into Eq. (2) under the open-circuit condition because $V_{OC} \ll J_{SC}AR_P$ as shown in Table I.

$$V_{OC} = \frac{nk_BT}{e}\ln\left[1+\frac{J_{SC}}{J_0}\left(1-\frac{V_{OC}}{J_{SC}AR_P}\right)\right] \approx \frac{nk_BT}{e}\ln\left(\frac{J_{SC}}{J_0}\right). \quad (2)$$

This equation suggests that V_{OC} is independent of R_P, which is too large to affect V_{OC}, but rather dependent upon n, J_{SC}, and J_0. As shown in Table I, the decrease in n contradicts the increase in V_{OC}, and the increase in J_{SC} is negligible compared to the two orders of magnitude decrease in J_0. We therefore conclude that the improvement in V_{OC} is mainly ascribed to the significant reduction in J_0 by postannealing. There should be no significant difference in blend morphology of the active layer between the pre and postannealed devices because the annealing temperature and time are the same; indeed there was no significant difference in absorption spectra between these two devices (not shown), but the interface between the active layer and the Al electrode is most likely to be different.

To investigate the dependence of the surface composition of the active layer at the Al interface on the annealing procedure, we measured the XPS spectra of a different surface area of the same P3HT/PCBM blend film. For the preannealed device, the blend surface without the Al deposition was measured after the thermal annealing. For the postannealed device, the blend surface was measured after the removal of the Al electrode that was deposited before the thermal annealing. Figure 2 shows S $2p$ spectra of the top surface of the pre and postannealed devices. The S $2p$ intensity of the postannealed device was about half that of the preannealed device, indicating that PCBM concentration at the Al interface is relatively enhanced in the postannealed device. Table II summarizes the atomic ratio of carbon to sulfur and the weight fraction of P3HT and PCBM for the pre and postannealed devices. Note that similar results were obtained in three independent measurements. As shown in Table II, the weight fraction of P3HT at the preannealed surface was as high as 69%, which is indicative of surface segregation of P3HT. The relatively high P3HT concentration at the preannealed surface is consistent with previous studies; 74% evaluated by XPS analysis[6] and 75%–80% evaluated by near-edge x-ray-absorption fine structure partial electron yield.[7] Such surface segregation of P3HT is rationally explained in terms of the surface energy: P3HT with a relatively low surface energy[11] is likely to segregate to the air surface. In other words, there exists undesirable contact between surface-segregated P3HT and the Al cathode in the preannealed device as shown in Fig. 3, which would cause the hole leakage to the Al electrode and hence increase J_0 and reduce V_{OC}.[12]

On the other hand, as shown in Table II, the weight fraction of PCBM at the postannealed surface was as high as 72%, which is indicative of surface segregation of PCBM instead. This compositional change at the Al interface is also rationally explained in terms of the surface energy as follows: PCBM with a relatively high surface energy[3] is likely to segregate to the Al electrode because metal has a surface energy generally much higher than organic materials.[13] Recently, similar surface segregations have been reported for blend devices of P3HT and poly((9,9-dioctylfluorene)-2,7 - diyl - alt- [4,7 - bis (3 - hexylthiophen - 5 - yl) - 2,1,3-benzothiadiazole]-2′,2″-diyl) (F8TBT).[4] In P3HT/F8TBT blend devices, the surface composition of F8TBT is only 5%

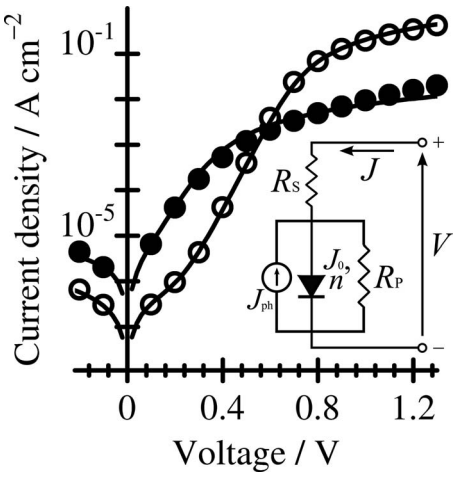

FIG. 1. Log plots of the current density of the preannealed device (●) and postannealed device (○) in the dark against voltage. The solid lines are fitted to the points with Eq. (1).

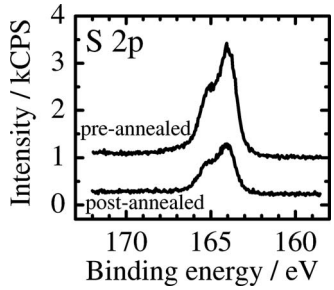

FIG. 2. The XPS spectra of S $2p$ obtained from the top of P3HT/PCBM blend films.

TABLE II. Atomic and weight ratios of the surface composition in P3HT/PCBM blend films.

	Atom (%)		Weight (%)	
Anneal	C 1*s*	S 2*p*	PCBM	P3HT
Pre	94	6	31	69
Post	98	2	72	28

for a blend film annealed without top electrode and increases to 15% for a blend film annealed after the electrode deposition because of a relatively high surface energy of F8TBT. In contrast, PCBM molecules occupy more than 70% at the Al interface of the P3HT/PCBM blend device after postannealing. This is probably because the diffusion constant of small molecules such as PCBM is much larger than that of polymer chains. Such surface-segregated PCBM would result in desirable contact to extract photogenerated electrons from PCBM and block the hole leakage from P3HT to the Al electrode. Therefore, the surface segregation of PCBM would lead to the dark carrier recombination between P3HT and PCBM in the blend layer whereas undesirable contact of P3HT to the Al electrode would cause the dark carrier recombination between P3HT and Al at the interface dominantly as shown in Fig. 3. The electron affinity of PCBM (3.9 eV) (Ref. 14) is smaller than the work function of Al (4.2 eV).[15] Thus, the surface segregation of PCBM is likely to reduce J_0 effectively, because J_0 exponentially decreases with the energy difference between holes and electrons at the recombination interface.[10,16] Indeed, even a small change in the energy difference only by 0.1 eV can reduce J_0 by about two orders of magnitude. We therefore conclude that the significant improvement in V_{OC} observed for P3HT/PCBM devices is primarily due to the surface segregation of PCBM at the Al interface induced by postannealing. More specifically, the postannealed P3HT/PCBM devices have a desirable interfacial structure at the Al interface contrary to previous reports.[5–8]

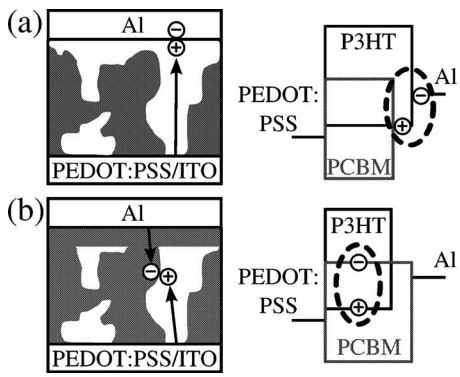

FIG. 3. The schematic illustration of surface segregation of P3HT/PCBM blend films (left) and the energy diagrams and major recombination interface (right). (a) Preannealed device and (b) postannealed device. The white and gray areas represent P3HT and PCBM domains, respectively.

In summary, P3HT/PCBM blend solar cells exhibited substantially enhanced V_{OC} by thermal annealing after the Al deposition compared to the preannealed device. The *J-V* characteristics of the device showed that J_0 is decreased by two orders of magnitude by the postannealing, which results in the improvement in V_{OC}. The XPS measurements revealed that the surface fraction of PCBM at the interface between the active blend layer and the Al electrode is as low as 31% in the preannealed device but is enhanced to 72% in the postannealed device. This shows that there exists a surface-segregated PCBM rich layer at the Al interface in the postannealed device, which can effectively prevent the hole leakage from P3HT to Al and hence reduce J_0 due to the dark carrier recombination at the interface. This finding suggests that P3HT/PCBM blend solar cells have a desirable hole-blocking layer due to the surface segregation of PCBM at the Al interface induced by postannealing, which is the origin of the significant improvement in V_{OC}.

This work was conducted at the Kyoto-Advanced Nanotechnology Network supported by "Nanotechnology Network" of the Ministry of Education, Culture, Sports, Science and Technology (MEXT), Japan, and partly supported by the JST PRESTO program (Photoenergy Conversion Systems and Materials for the Next Generation Solar Cells) and the Global COE program (International Center for Integrated Research and Advanced Education in Materials Science) from MEXT, Japan.

[1] C. J. Brabec and J. R. Durrant, MRS Bull. **33**, 670 (2008).
[2] G. Dennler, M. C. Scharber, and C. J. Brabec, Adv. Mater. **21**, 1323 (2009).
[3] C. M. Björström, A. Bernasik, J. Rysz, A. Budkowski, S. Nilsson, M. Svensson, M. R. Andersson, K. O. Magnusson, and E. Moon, J. Phys.: Condens. Matter **17**, L529 (2005).
[4] C. R. McNeill, J. J. M. Halls, R. Wilson, G. L. Whiting, S. Berkebile, M. G. Ramsey, R. H. Friend, and N. C. Greenham, Adv. Funct. Mater. **18**, 2309 (2008).
[5] M. Campoy-Quiles, T. Ferenczi, T. Agostinelli, P. G. Etchegoin, Y. Kim, T. D. Anthopoulos, P. N. Stavrinou, D. D. C. Bradley, and J. Nelson, Nature Mater. **7**, 158 (2008).
[6] Z. Xu, L. Chen, G. Yang, C. Huang, J. Hou, Y. Wu, G. Li, C. Hsu, and Y. Yang, Adv. Funct. Mater. **19**, 1227 (2009).
[7] D. S. Germack, C. K. Chan, G. H. Hamadani, L. J. Richter, D. A. Fischer, D. J. Gundlach, and D. M. Delongchamp, Appl. Phys. Lett. **94**, 233303 (2009).
[8] L. Chen, Z. Hong, G. Li, and Y. Yang, Adv. Mater. **21**, 1434 (2009).
[9] Y. Zhao, Z. Xie, Y. Qu, Y. Geng, and L. Wang, Synth. Met. **158**, 908 (2008).
[10] W. J. Potscavage, A. Sharma, and B. Kippelen, Acc. Chem. Res. **42**, 1758 (2009).
[11] J. Jaczewska, I. Raptis, A. Budkowski, D. Goustouridis, J. Raczkowska, M. Sanopoulou, E. Pamula, A. Bernasik, and J. Rysz, Synth. Met. **157**, 726 (2007).
[12] N. Li, B. E. Lassiter, R. R. Lunt, G. Wei, and S. R. Forrest, Appl. Phys. Lett. **94**, 023307 (2009).
[13] H. L. Skriver and N. M. Rosengaard, Phys. Rev. B **46**, 7157 (1992).
[14] K. Kanai, K. Akaike, K. Koyasu, K. Sakai, T. Nishi, Y. Kamizuru, T. Nishi, Y. Ouchi, and K. Seki, Appl. Phys. A: Mater. Sci. Process. **95**, 309 (2009).
[15] *CRC Handbook of Chemistry and Physics*, 80th ed., edited by D. R. Lide (CRC, New York, 1999).
[16] W. J. Potscavage, Jr., S. Yoo, and B. Kippelen, Appl. Phys. Lett. **93**, 193308 (2008).